SYNTHESIS AND CHARACTERIZATION OF CdO_{1-x} ZnO_x FOR SOLAR CELL APPLICATIONS

R. A. AHMED[a], A. J. NOORI[b], I. M. IBRAHIM[c*] , E. S. IBRAHIM[d]
[a]*General Directorate of Education Salahudin, Education department of Tuz,*
[b]*Directorate of Kirkuk province Education*
[c]*Department of Physics, College of Science, University of Baghdad, Baghdad, Iraq*
[d]*General Directorate of Education Salahudin, Education department of Dhulueaa*

In this work, CdO_{1-x} ZnO_x with (x= 5and 25%) have been deposited on glass and Si substrates by chemical spray method, thin films were examined by x-ray diffractometer (XRD) which showed the films are polycrystalline also the attendance of the CdO cubic shaped and hexagonal Zinc oxide (ZnO) phases at x concentration 5% and 25% . The grain size decrease with expansion of ZnO content. The surface morphology of the samples showed densely packed grains. Optical absorption shows the effect of ZnO doping on band gap of CdO where the optical Absorption varies from 33% to 70% and the band gap various from 2.74 to 3.14 eV. Under 30mW/cm^2 intensity illumination photovoltaic properties were examined. An open Circuit voltage (V_{oc}) increase and a fill factor (F.F.) increase with increase of x concentration . The reversed bias capacity was calculate like a versus to reverse bias voltage at frequency 1 MHz. It also indicates that heterojunction was abrupt. The built in voltage increase with the increasing of x content.

(Received September 16, 2018; Accepted January 7, 2019)

Keywords: Thin films, Photovoltaic, Fill factor, Metal oxide

1. Introduction

Solar cells applications used widely by Transport conducing Oxide (TCO). Cadmium Oxide (CdO) and Zinc oxide (ZnO) have higher degree of clearance in the observable area of the electromagnetic spectrum; they showed n-type conductivity because of Oxygen vacancies [1]. Almost all of the TCO samples have n-type in conduction which is selecting a wide band gab Oxide attained in a higher clearance with functional electrical conduction. CdO have the respective low innate band space [2] which can get to high band space cost owing to its lower potent transporter accumulation [3]. It is also lead to large moving due to action of doping.

ZnO is a direct wide band space semiconductor substance of class (II – VI) with a hexagonal quartzite structure. Zinc oxide own special electrical and visual effects, such as a broad energy gap (3.37ev) at room temperature and a large size of a mobile excited state with energy of 60 meV which can produce an important allocation detention effect [4].

Both of the low resistivity and the high visual transmission in the visible limit make Zinc oxide significant structure in the form of heat mirrors which used in gas cooking stove conduction coating air-crafts and glass avoiding surface icing .Variety of depositions skills have used widely to form Zinc oxide and doped Zinc oxide fine film, such as sputtering [5], spray pyrolysis [6-9] and sol-Gel method [10-13]. Of these methods spray pyrolysis is the most simplest method and very effective.in this work we aim to study the effect of Zn concentration on the characteristics of structural, absorption spectrum and solar cell efficiency.

*Corresponding author: dr.issamiq@gmail.com

2. Experimental work

Chemical transformation mechanism prepared $CdO_{1-x}ZnO_x$ samples deposited on glass and p-type Silicon Si(111) substrates at heating temperature (350 ^{0}C). Dissolving Cadmium Chloride [CdO Cl_2. H_2O] and Zinc Acetate [$Zn(CH_3COO)_2.2H_2O)_4$] prepared spray solution. The above solution was placed in the flask of the atomizer and spread by controllable pressurized Nitrogen gas flow on the heated substrates. The optimum experimental conditions for obtaining homogeneous $CdO_{1-x}ZnO_x$ films at (350 ^{0}C) had been resolute by time , the spraying time was also 4 seconds that directed by modifiable coil heated subtracts and the last one left for 12 seconds and after each spraying management the deposited samples leave to dry . Laser interferometer measured the thickness of the prepared films which about to 100 nm.

3. Results and discussion

3.1. Structural bending

X-ray diffractometer is a powerful and nondestructive methods for material's assuming that the crystal structure, orientation and also grain size can be determined, in which examined by using Philips PW X-ray diffractometer system, Bragg's law can measure the interplaner distance for different plane [14].

$$n\,\lambda = 2\,d\,sin\theta \tag{1}$$

Where n: is an number (1, 2, 3, ….) that represents the order of the interface, λ: is the X-ray wave length, d: is the interplaner distance and θ: represent the include angle. The average grain size (which resemble D in the below) of crystallized structures have main function for determining the properties of the material that can be obtained from the spectrum of X-ray by calculating full width at half maximum *(FWHM),*which is given by Scheror's relation [15]:

$$\mathrm{D} = \frac{0.9\lambda}{\beta\,cos\,\theta} \tag{2}$$

Where 0.9 is a correction factor, β: represents the amount of curved width at the middle of a maximum peak in radian.

The X-ray diffractometer is resemble as a patterns of the deposited $CdO_{1-x}ZnO_x$ films with x concentration (x= 5 , 25%) on glass at substrate temperature equal to 350°C with thickness equal to about 100 nm. Figure (1) shows the XRD patterns of CdO_{1-x} ZnO_x films which indicate that the samples are polycrystalline structure and the films have a mixture of a hexagonal structure for CdO and a cubic structure for ZnO according to American standardization of testing materials (ASTM) card. Table (1) lists the observation of the interplaner distance values with standard (JCPDS-ICDD file number 96-900-6674, and 96-230-0113 for CdO and ZnO compound. XRD patterns for fine films exhibits the increase in the (*FWHM*) which indicates a decreasing in the grain size of $CdO_{1-x}ZnO_x$ thin films, depending on Scherer's relation, equation (2), where the relation between the grain size and (*FWHM*) is reversal.

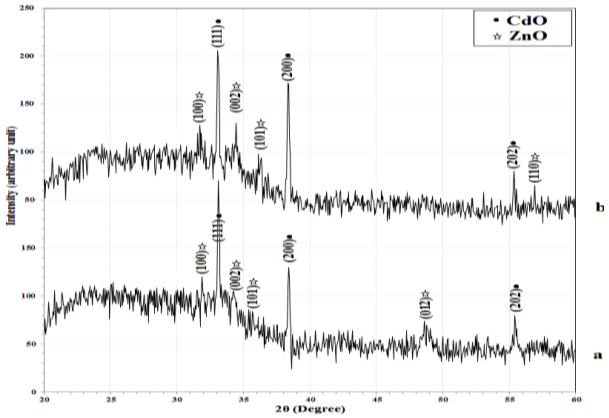

Fig. 1. XRD patterns for CdO_{1-x} ZnO_x thin film (a) x= 5%, (b) x= 25%.

Table 1. Show the Parameters of Structure with interplaner distance and grain size of CdO_{1-x} ZnO_x films in different x.

$CdO_{1-x}ZnO_x$	2 Theta (Degree.)	$FWHM$	d_{hkl} (Å) Exp.	D (Å)	d_{hkl}(Å) Standard.	hkl	structure	Card number.
x= 5%	31.8828	0.3905	2.8046	21.2	2.8141	(100)	Cub.ZnO	96-230-0113
	33.1102	0.1674	2.7034	49.5	2.7078	(111)	Hex.CdO	96-900-6674
	34.2259	0.3905	2.6178	21.3	2.6027	(002)	Cub.ZnO	96-230-0113
	35.6206	0.3905	2.5184	21.4	2.4755	(101)	Cub.ZnO	96-230-0113
	38.4100	0.2232	2.3417	37.7	2.3450	(200)	Hex.CdO	96-900-6674
	48.6192	0.8926	1.8712	9.8	1.9107	(012)	Cub.ZnO	96-230-0113
	55.4254	0.3905	1.6564	23.0	1.6582	(202)	Hex.CdO	96-900-6674
x= 25%	31.7155	0.3905	2.8190	21.1	2.8141	(100)	Cub.ZnO	96-230-0113
	33.0544	0.2232	2.7078	37.1	2.7078	(111)	Hex.CdO	96-900-6674
	34.4491	0.5579	2.6013	14.9	2.6027	(002)	Cub.ZnO	96-230-0113
	36.2343	0.4463	2.4772	18.7	2.4755	(101)	Cub.ZnO	96-230-0113
	38.3543	0.2232	2.3450	37.7	2.3450	(200)	Hex.CdO	96-900-6674
	55.3696	0.3347	1.6580	26.8	1.6582	(202)	Hex.CdO	96-900-6674
	56.9317	0.1674	1.6161	54.0	1.6247	(110)	Cub.ZnO	96-230-0113

Atomic force microscopy (AFM) is known the regarded as one of the best methods for the analysis of external layers because of the high resolution and the software's power analysis. Atomic force microscopy used the $CdO_{1-x}ZnO_x$ thin films morphologically which characterized. In the extreme situations of the fine films the rough of surface may be due to the film thickness and this could affect all the film possessions such as magnetically, optical also electrical properties and mechanical.

Fig. (2) Shows the CdO_{1-x} ZnO_x samples with different x centralization precipitate at 350 ^oC of temperature. It also can know which sample are densely store, uniform and pinhole unlimited and it seems to be that the external appearance of these samples have larger number of size of grain and they're spread homogeneously , and that mean the crystallization nature of the sample . First optical tastings of the deposited sample have illustrated that they're dense and have good attachment to the substrate and cracking wasn't noticed. The grains are made of variable size which start from 88-29nm to 87.02 nm. However, on the other hand the grains sizes are observed

to decrease while the ZnO ratio is increase and the table (2) is show this , which depend on Atomic force microscopy image Fig. (2). The grain density diminished and showing the smaller size grains clustered together to form grains which are smaller of CdO and ZnO. Also the average roughness (S_a) and root mean square of roughness surface (S_q) of the samples [see Table 2. The (S_a) and (S_q) evaluation get rise with getting rise in ZnO concentration and this mean a reducing in the grain size of as its shown in Table 2 and Fig. 2. These reduction of evaluation of (S_a) and (S_q) explain that the a reduction in the reflection of light and increase in the absorption of light of the optical area in the spectrum of solar cells.

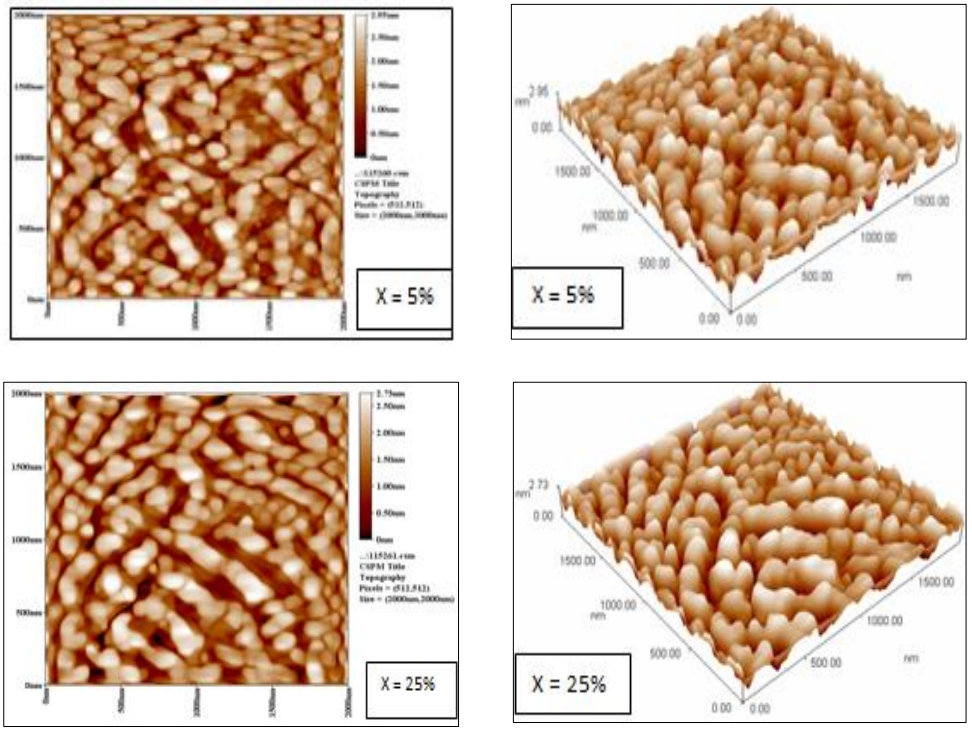

Fig. 2. AFM image of CdO_{1-x} ZnO_x thin films at x= 5% and x= 25%.

Table 2. Shows the grain size, S_a, and Sq. from AFM for CdO_{1-x} ZnO_x thin films.

CdO_{1-x} ZnO_x	Grain size (nm)	average roughness (S_a) (nm)	Root mean square (S_q) (nm)
x = 5%	88.29	0.474	0.577
x = 25%	87.03	0.488	0.588

3.2. The energy band gap

The optical absorbance spectra of CdO_{1-x} ZnO_x films with different x content were measured using UV/ Visible SP –8001 spectrophotometer over the range 300–1100 nm. Fig. (3) show the absorption spectra of the films and that all samples exhibit absorption edge which are blue shifted. The optical absorption edge can analyze by the Tauc equation [16]:

$$\alpha h\nu = A(h\nu - E_g)^m \quad (3)$$

Where A is a constant, m value is ½ and 2 for direct and indirect transitions respectively. Because of not being sharp increasing in transmission spectra near the absorption edge of CdO_{1-x} ZnO_x thin film direct allowed band gaps were also determined. So, direct allowed band gap of the CdO_{1-x} ZnO_x thin films were determined by Tauc plots f ($h\nu$)= $(\alpha h\nu)^2$ [12]. Fig. (4) shows the Tauc plots

for CdO_{1-x} ZnO_x thin films. The direct allowed band gaps of the thin films (2.74 and 3.14) eV respectively for x (0.05 and 0.25). These data show the effect of ZnO doping on band gap values of CdO films and possibility of wavelength tenability by preparing films of alloy CdO_{1-x} ZnO_x.

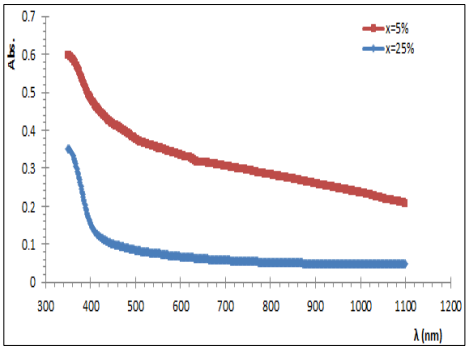

Fig. 3. Absorbance Spectra of CdO_{1-x} ZnO_x films with range x (5% to 25%).

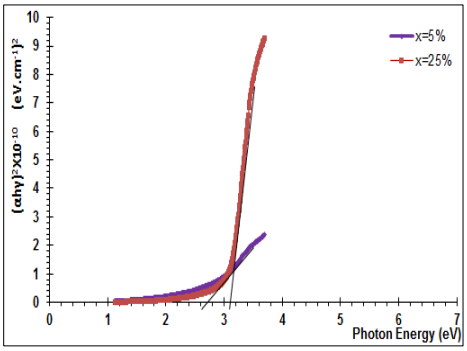

Fig. 4. The vs. photon energy for CdO_{1-x} ZnO_x films with range x (5% to 25%).

3.3. Characteristics of current - Voltage CdO_{1-x} ZnO_x/p-Si heterojunction

To decisive characterization of the photovoltaic of the $CdO_{1-x}ZnO_x$ /p-Si (111), the feature of current - voltage of the samples in a dark and lighting situations were examined as shown in Fig. 6. A good correction ways had shown under darkness situations of the improved heterojunction. The current of the darkness getting rise with rising the applied voltage. In the reverse bias case the current rises with lighting potency of 30 mW/cm^2 and the diodes give a maximum open circuit voltage (V_{oc}) of 0.15 V , 0.28V and short-circuits current (I_{sc}) of 0.05 µA , 0.018 µA for x= 5% and x=25% respectively. These numbers are indication of the n- CdO_{1-x} ZnO_x/p-Si diodes exhibit a photovoltaic performance, because the photovoltaic has effectiveness include forming of current and voltage in a p–n heterojunction on the subjection to potency of lighting. The Filling factor (FF) was accounting from Fig. 5 by using this equation [17].

$$FF = \frac{I_{max}\ V_{max}}{I_{sc}\ \ V_{oc}} \qquad (4)$$

Where I_{max} is the maximum current and V_{max} is the maximum voltage in which the power is at maximum output and P_{in} is the input of the power to the cell and its clarify as the total energy of radiant occurs on the external layers of the cell.

The I_{max} and V_{max} values were found to be 0.03 µA and 0.09 V for x= 5% and 0.012 µA and 0.14V for x=25%. Because of the low value of the existence of higher sequences resistant the calculated fill factor were 0.30 plus 0.33 for X=5%, X=25% respectively.

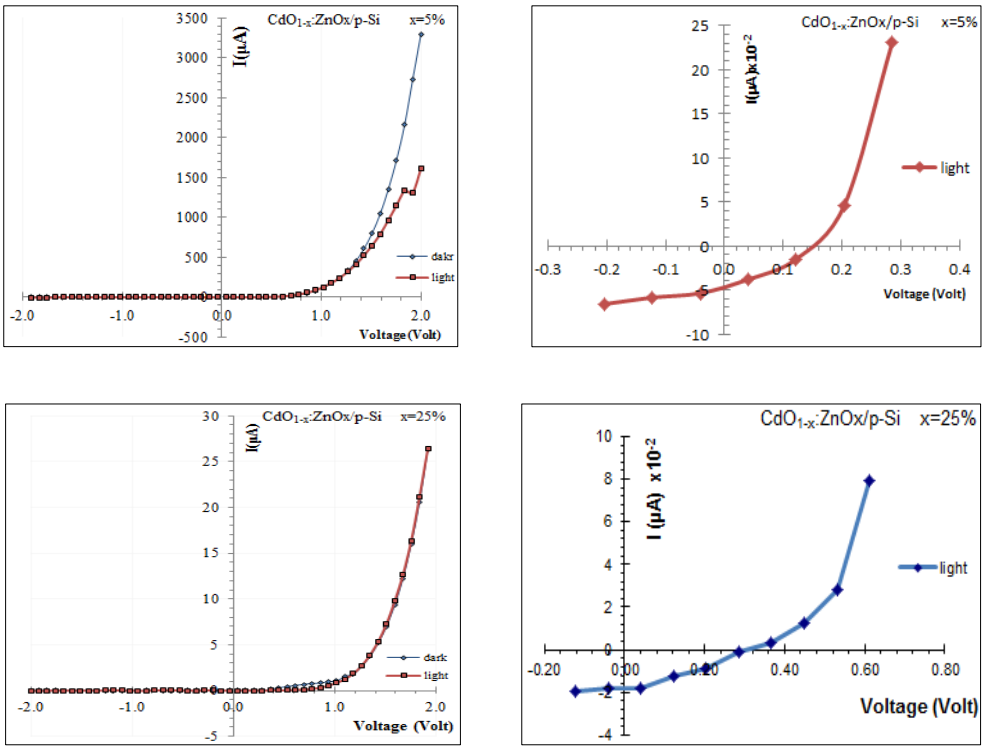

Fig. 5. I - V characteristics for $CdO_{1-x}ZnO_x$ /p- Si Heterojunction at different x content.

Table 3. Values of I-V parameters and ideality factor CdO_{1-x}: ZnO_x /p- Si Heterojunction at different x content.

CdO_{1-x} ZnO_x /p- Si	I_{sc} (μA)	V_{oc} (V)	I_m (μA)	V_m(v)	F.F	β
X = 5%	0.05	0.15	0.03	0.09	0.30	2.59
X = 25%	0.018	0.280	0.012	0.140	0.333	3.231

3.4. C-V characteristics of $CdO_{1-x}ZnO_x$/p-Si Heterojunction

Capacitance-Voltage characteristics (C-V) have been measured for $CdO_{1-x}ZnO_x$/ *p- Si* heterojunction which prepared with difference x concentration at substrate temperature 350ºC as the means of determining the built-in potential. The capacitor measuring of the heterojunction as a role of the reversed biasing voltage in a span (-0.02 to -2) Volt were performed in dark at room temperature using a WK 6440B LCR meter computerized. The test frequency was set at 1 MHz.

Anderson shows that the join capacitor per a element area, for an abrupt anisotype heterojunction can write as [18]:

$$\frac{1}{C^2} = \left[\frac{2\varepsilon_p N_p + 2\varepsilon_n N_n}{qN_p N_n \varepsilon_n \varepsilon_p}\right].(V_D - V) \qquad (7)$$

Where ε_p and ε_n are the dielectric constants of n and p type semiconductors respectively, N_p and N_n are the concentrations of the acceptor and donor, V_{bi} is the built-in potential of the junction, and V_a is the voltage which was applying. From this you can see a plot of (A/C^2) against applied reverse voltage V_a is linear and its extrapolated to cross the voltage axis gives the built-in potential of the junction V_{bi} as given in Fig. 6, and the reverse change of the experimental curve (A/C^2) as a function of voltage gives an indication of the presence of abrupt hetrojunction. The plots indicated

straight line relationship it means that the junction is of an abrupt type. The interception of the straight line with the voltage axis at (A/C^2)= 0, which represents the built – in voltage. V_{bi}, can be seen from the same figure which values 0.85 eV and 1.15 eV for x= 5% and 25% respectively, which increases with increase in x concentration of the hetrojunction because increase of energy gap with increase ZnO concentration.

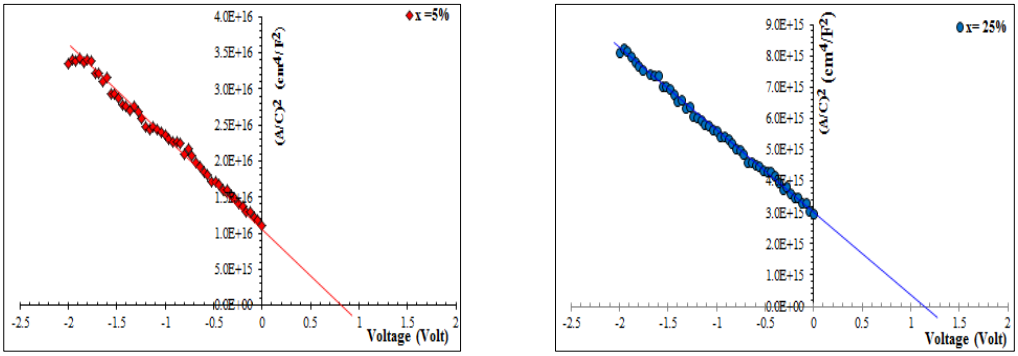

Fig. 6. The relationship between A/C^2 and the reverse bias voltage for CdO_{1-x} ZnO_x /p- Si heterojunction with different x content.

4. Conclusions

In this work the CdO_{1-x} ZnO_x films that deposited on glass and P- Si substrates is prepared by chemical spray pyrolysis successfully . The X-ray diffraction demonstrated the film was multi-crystalline structure. The architecture of AFM samples have large unit of grain size and a homogeneous distributing and unified, that show the crystallized style of the sample. A grain size of deposited films determined to be 88.29 and 87.03 nm at ***x*** = 5% , 25%. The direct energy gap of $CdO_{1-x}ZnO_x$ films were found increase with increase ***x*** content. C-V measurements which revealed an abrupt heterojunction and show an increasing of V_{bi} with increasing doping for all samples. I-V characteristic under a 30 mW/cm^2 illumination show the fill factor of (n- CdO_{1-x} ZnO_x /p-Si) were found increase with increasing *x* contents.

References

[1] A. Boeeze, P. G. Perkins, Solid State Physics **13**, 1031 (1973).
[2] R. J. Deokate, S. V. Salunkhe, G. L. Agawane, B. S. Pawar, S. M. Pawar, K. Y. Rajpure, A. V. Moholkar H. Kim, J. Alloys Compd. **496**, 357 (2010).
[3] S. Jin, Y. Yang, J. E. Medvedeva, L. Wang, S. Li, N. Cortes, J. R. Ireland, A. W. Metz, J. Ni, M. C. Hersam, A. J. Freeman, T. J. Marks, Chem. Mater. **20**, 220 (2008).
[4] W. W. Wenas, A. Yamada, K. Takahashi, M. Yoshino, M. Konagai, J. Appl. Phys. **70**, 7119 (1991).
[5] Shoubin Xue, Huizhao Zhuang, Chengshan Xue, Shuyun Teng, Lijun Hu, Eur. Phys. J. Appl. Phys. **36**, 1 (2006).
[6] O. Vigil, F. Cruz, G. Santana, L. Vaillant, A. Morales-Acevedo, G. Conteras-Puent, Thin Solid Films **361-362**, 53 (2000).
[7] G. Santana, O. Vigil et. al., Thin Solid Films **373**, 235 (2000).
[8] Y. Caglar, S. Ilican, M. Caglar, Physic(a) **394**, 86(2007).
[9] A. Ortiz, E. P. Zironi, J. Rickards et.al., Thin Solid Films **333**, 196 (1998).
[10] R. Siddeswaran, R. Sankr, P. Sureshkumar et.al., Crys. Res. Technol. **41**(5), 446 (2006).
[11] G. C. Psarras, S. Baskoutas et.al., Phys. Stat. Sol(a) **205**(8), 2033 (2008).
[12] M. Ohyama, H. Kazuka, T. Yoko, Thin Solid Films **306**, 78 (1997).
[13] K. Uma, M. Rusop, T. Soga, T. Jimbo, Japanese Journal of Applied Physics **46**(5) 40-44.

[14] M. Thakurdesai, N. Kukarni, B. Chalke, A. Mahadkar, Calcogenide Letters **8**(3), 223 (2011).
[15] Y. Sitrotin, M. Shaskolskaya, Mir publishers, Moscow, "Fundamental of crystal physics", (1982).
[16] S. Ilican, F. Yakuphanoglu, M. Caglar, Y. Caglar, J. Optoelectron. Adv. M. **9**(7), 2180 (2007).
[17] M. S. Inpasalini, R. G. Devi, D. Balamurugan, B. G. Jeyaprakash, J. B. B. Rayappan, Journal of Applied Sciences **16**, 1742 (2012).
[18] Abdalla A. Alnajjar A, Maysoon F. A. B. Alias, B. Rasha Almatuk, Ala A. J. AlDouri, Renewable Energy **34**, 2160 (2009).